1994-08

# Neural Control of Interlimb Oscillations I: Human Bimanual Coordination

Grossberg, Stephen

Boston University Center for Adaptive Systems and Department of Cognitive and Neural Systems

# NEURAL CONTROL OF INTERLIMB OSCILLATIONS I. HUMAN BIMANUAL COORDINATION

Stephen Grossberg, Christopher Pribe, and Michael A. Cohen

July 1994
Revised: May 1996

Technical Report CAS/CNS-94-021



Boston University Center for Adaptive Systems and
Department of Cognitive and Neural Systems
677 Beacon Street
Boston, MA 02215

# NEURAL CONTROL OF INTERLIMB OSCILLATIONS I: HUMAN BIMANUAL COORDINATION

by

Stephen Grossberg‡, Christopher Pribe§, and Michael A. Cohen†
Center for Adaptive Systems
and
Department of Cognitive & Neural Systems
Boston University
677 Beacon Street
Boston, MA 02215

July 1994
Revised: May 1996

Technical Report CAS/CNS-TR-94-021

Requests for reprints should be sent to:
Stephen Grossberg
Department of Cognitive and Neural Systems
Boston University
677 Beacon Street, Room 201
Boston, MA 02215
(617) 353-9481

Running Head: *Human Bimanual Oscillations*

---

‡ Supported in part by the Air Force Office of Scientific Research (AFOSR F49620-92-J-0499 and AFOSR F49620-92-J-0225), the National Science Foundation (NSF IRI-90-24877), and the Office of Naval Research (ONR N00014-92-J-1309).

§ Supported in part by the Army Research Office (ARO DAAL03-88-K-0088), the Advanced Research Projects Agency (AFOSR 90-0083), the National Science Foundation (NSF IRI-90-24877), and the Office of Naval Research (ONR N00014-92-J-1309).

† Supported in part by the Air Force Office of Scientific Research (AFOSR 90-0128 and AFOSR F49620-92-J-0225).

Acknowledgements: The authors wish to thank Carol Jefferson and Robin Locke for their valuable assistance in the preparation of the manuscript.

## ABSTRACT

How do humans and other animals accomplish coordinated movements? How are novel combinations of limb joints rapidly assembled into new behavioral units that move together in in-phase or anti-phase movement patterns during complex movement tasks? A neural central pattern generator (CPG) model simulates data from human bimanual coordination tasks. As in the data, anti-phase oscillations at low frequencies switch to in-phase oscillations at high frequencies, in-phase oscillations occur both at low and high frequencies, phase fluctuations occur at the anti-phase in-phase transition, a "seagull effect" of larger errors occurs at intermediate phases, and oscillations slip toward in-phase and anti-phase when driven at intermediate phases. These oscillations and bifurcations are emergent properties of the CPG model in response to volitional inputs. The CPG model is a version of the Ellias-Grossberg oscillator. Its neurons obey Hodgkin-Huxley type equations whose excitatory signals operate on a faster time scale than their inhibitory signals in a recurrent on-center off-surround anatomy. When an equal command or GO signal activates both model channels, the model CPG can generate both in-phase and anti-phase oscillations at different GO amplitudes. Phase transitions from either in-phase to anti-phase oscillations, or from anti-phase to in-phase oscillations, can occur in different parameter ranges, as the GO signal increases.



**Key Words:** Central pattern generator, oscillations, neural network, gait, coordination, motor cortex, GO signal, lateral inhibition.

## TABLE OF CONTENTS

## 1. In-Phase and Anti-Phase Bimanual Coordination

Humans and other animals effortlessly control their limbs to accomplish coordinated movements. In particular, novel combinations of joints can be rapidly assembled into new behavioral units, or synergies, that are capable of moving together in in-phase or anti-phase movement patterns to carry out complex movement tasks like tool use, dancing, piano playing, and the like. In order to study this competence, an experimental paradigm has previously been developed in which humans are asked to move fingers from both hands at variable frequencies and to do so in in-phase or anti-phase rhythms. Data from these experiments exhibit characteristic properties which provide clues to how new combinations of joints can be rapidly bound together to generate coordinated movement patterns.

This article describes a neural network model that suggests how novel joint combinations can be rapidly bound together in rhythmic patterns. These patterns are emergent properties due to network interactions. They are not explicitly represented or programmed in the network. The model simulates parametric properties of human movement data as emergent, or interactive, properties of nonlinear network interactions. This network takes the form of a central pattern generator (CPG) that coordinates the movement across limb joints when volitional input signals perturb the network.

For example, in a bimanual finger tapping task, Yamanishi *et al.* (1980) required subjects to tap keys in time to visual cues. The timing of the cues was varied across ten relative phases: $(0.0, 0.1, 0.2, \ldots 1.0)$, where $0.0 = 0°$ and $1.0 = 360°$. The authors observed two properties in the responses of their subjects. First, the subjects' fingers tended to slip from intermediate relative phase relationships toward purely in-phase (0.0 and 1.0) or anti-phase (0.5) relationships. Second, the observed in-phase and anti-phase oscillations exhibited less variability than intermediate phase relationships. That is, when the subjects were asked to synchronize to signals whose phase relationships varied from 0.0 to 1.0, the standard deviation of the errors was lowest when the phase relationship was near in-phase (0.0 and 1.0) or pure anti-phase (0.5). The standard deviation of the errors increased as the subjects were required to move away from the in-phase or pure anti-phase oscillations. These two properties were also observed by Schoner and Kelso (1988) and by Tuller and Kelso (1989). The appearance of the plot of the standard deviation of the errors has been called the "seagull effect" (Tuller and Kelso, 1989); see Figure 1A. The CPG model exhibits the seagull effect, as well as the slip toward pure in-phase and pure anti-phase oscillations (Figure 1B).

Figure 1

Kelso (1981) described a related experimental task in bimanual coordination which involved moving fingers or limbs in in-phase or anti-phase oscillations. For example, adduction of the right index finger simultaneously with abduction of the left index finger is an anti-phase movement. Concurrent abduction (or adduction) of both fingers is an in-phase movement. The rate of movement of the fingers was signaled by a metronome. The following fundamental qualitative behaviors emerge from the body of the bimanual finger movement data for normal subjects:

(1) Subjects are capable of producing a variety of relative phases at low frequencies. However, the underlying oscillation generation mechanism is biased in favor of in-phase and anti-phase relationships (Yamanishi *et al.*, 1980) as shown by the "seagull effect" described above and by a tendency to slip from intermediate phase relationships toward in-phase or

anti-phase relationships.

(2) Subjects are capable of performing purely in-phase movements at both low and high frequencies for bimanual wrist movements (Kelso, 1984) and for bimanual finger movements, (Tuller and Kelso, 1989).

(3) Subjects do not have complete conscious control over their movements under the conditions of the bimanual coordination experiments. In particular, though subjects could perform anti-phase movements at low frequencies, they exhibited a spontaneous switch to an in-phase relationship at higher frequencies (Kelso, 1984).

(4) The relative phase of the movement produced by the subject often fluctuates during a spontaneous switch from anti-phase to in-phase movements (Kelso, 1984; Kelso and Scholz, 1985).

Figure 2

The CPG model reliably reproduces all four effects in our simulations; see Figures 2 and 3. In order to simulate these four properties, the model was presented with a pulsed wave anti-phase oscillatory input to each channel, as shown in Figure 2A. These pulsed inputs represent the descending volitional commands to move the fingers as required. The square waves were either equal to a constant input level when on, or set to zero when off. The input level and the duration of the "on" portion of the signal were held constant for each of the simulations. For each simulation, only the frequency of these pulses was varied. The duration of the "on" portion of the signals was 2.0 in all simulations. Shorter duration signals did not reliably produce oscillations in both channels. In order to generate Figure 2, we computed, for 145 points, the relative phases of the output signals using the times at which they exceeded a threshold. As the frequency was varied, the model showed a switch from anti-phase (Figure 2B) to in-phase (Figure 2D) oscillations. The system also exhibited fluctuations in which no clear phase relationship dominates in between these regimes (Figure 2C). As in the data, the reverse transition in response to in-phase inputs did not occur (Figure 3).

Figure 3

## 2. The CPG Model

The CPG uses ubiquitously occurring physiological mechanisms, notably model nerve cells, or cell populations, that obey membrane equations (Hodgkin, 1964), also called shunting equations (Grossberg, 1982). These neurons are connected by a recurrent on-center off-surround network, a design that is also ubiquitous in the nervous system (Grossberg, 1982; Kandel *et al.*, 1991; Kuffler, 1953; Ratliff, 1965; Von Békésy, 1968) and that has been used to explain other types of motor behavior (Pearson, 1993). In particular, the cells excite themselves via fast feedback signals while they inhibit themselves and other populations via slower feedback signals (Figure 4). Such slow inhibition is well-known to occur in sensory-motor systems; see for example Dudel and Kuffler (1961) and Kaczmarek and Levitan (1987). When a subset of model cells is driven by anti-phase inputs or by in-phase inputs of increasing frequency, as in Figures 2 and 3, then the network interactions generate observed properties of variable frequency finger movements as emergent properties of the entire network. Our main result is thus to show how the emergent properties of ubiquitous physiological and anatomical mechanisms give rise to behavioral properties of movement.

This approach is distinguished from models that are expressed directly in terms of operating characteristics of the data, such as the phase angle of the limbs (Kelso, Scholz, and Schöner, 1988; Schöner *et al.*, 1990; Yamanishi, Kawato, and Suzuki, 1980; Yuasa and Ito, 1990).

Figure 4

The Kelso data and our simulations suggest the prediction that this type of opponent CPG acts as a kind of nonlinear low pass filter; that is, at high frequencies of stimulation, the output of the system converges to the response obtained from the network when pulsed inputs are replaced by a tonically active nonspecific signal of the same amplitude that is input equally to all the cells. Such a nonspecific input may be called an arousal or GO signal. It represents the simplest type of volitional signal that can activate network oscillations. The model's ability to resolve a temporally changing input signal is inversely related to its frequency. Suppose that the model exhibits a prescribed phase response to a sustained GO signal. Then the output of the system converges to this response when increasing high frequency inputs of the same amplitude are used, irrespective of the phase relationships among the inputs. How such a GO signal influences model dynamics is thus studied below.

Before turning to a discussion of GO signal control, a remark about how afferent feedback may alter the present results is in order. Including an afferent feedback signal from the limbs, say from tactile sensations, proprioception, or joint receptors, may not necessarily improve the ability of such a CPG to stay phase-locked to a time-varying input signal. The afferent signal will either overlap in time with the input signal or it will not. If it does overlap, suppose for definiteness that it increases the amplitude of the input. Increased amplitude has not, in our simulations, improved the ability of the model to accurately follow the phase of the input. On the other hand, if the efferent signal lags the input, then this signal tends to increase the frequency of the total input to the oscillator, both afferent and efferent, and thus helps to favor the rhythm that would be generated by a tonically active GO signal.

In the limit of high input frequencies, afferent signals could alter the dynamics of the system, since the type of oscillation that is produced by a GO signal does depend upon its amplitude, as will be shown below. This effect, however, does not improve the system's ability to remain phase-locked to the input, since the amplitude of the GO signal, not the phase of the inputs, would determine the result.

GO signal control has been used in other models of biological motor control, notably models of how the brain controls variable-speed reaching behaviors (Bullock and Grossberg, 1988, 1991). In these models, the GO signal calibrates the speed of a phasic reaching movement by a limb such as an arm. In the present example, the GO signal calibrates movement speed by increasing oscillation frequency. The same GO signal can also trigger bifurcations between different oscillatory patterns, or gaits. Thus GO signal control is of interest for understanding both the high frequency movements in response to temporally oscillatory inputs as well as the gaits generated at all frequencies in response to temporally steady inputs. Whenever the volitional signal is realized by a single GO signal, we call the model a GO Gait Generator, or $G^3$ model.

## 3. The Ellias-Grossberg Oscillator

The $G^3$ model belongs to a more general class of CPG models that is closely related to the model of Ellias and Grossberg (1975). In the Ellias-Grossberg models, the excitatory signals but not the inhibitory signals are coupled to a membrane equation, or shunting,

interaction. We found it necessary for both the excitatory and the inhibitory signals to be coupled to shunting membrane processes to simulate all the data patterns that are presented below and in Pribe, Grossberg, and Cohen (1996). Such a CPG model obeys the equations

$$\frac{d}{dt}x_i = -Ax_i + (B - x_i)[f(x_i) + I_i] - (C + x_i)\sum_j D_{ij}g(y_j) \tag{1}$$

and

$$\frac{d}{dt}y_i = E[(1 - y_i)[x_i]^+ - y_i], \tag{2}$$

where

$$[\omega]^+ = max(\omega, 0) \tag{3}$$

and

$$f(\omega) = \frac{F_1([\omega]^+)^2}{F_2 + ([\omega]^+)^2},\ g(\omega) = \frac{G_1([\omega]^+)^2}{G_2 + ([\omega]^+)^2}. \tag{4}$$

In Hodgkin–Huxley notation, equation (1) is of the form

$$C\frac{\partial V}{\partial t} = (V^p - V)g^p + (V^+ - V)g^+ + (V^- - V)g^-, \tag{5}$$

where the variable voltage $V = x_i$, the constant saturation voltages $V^p = 0, V^+ = B$, and $V^- = -C$; and the conductances equal $g^p = A$, $g^+ = f(x_i) + I_i$, and $g^- = \sum_j D_{ij}g(y_j)$. In (1), $f(x_i)$ plays the role of a fast excitatory conductance and $g(y_j)$ of a slow inhibitory conductance. Terms $(B - x_i)$ and $(C + x_i)$ in (1) are shunting terms. Term $(1 - y_i)$ in (2) is a shunting term that was not used in the original Ellias and Grossberg (1975) study. The equation for the slow term $y_j$ in (2) can be rewritten in Hodgkin–Huxley form as

$$\frac{d}{dt}y_i = \alpha(x_i)[\beta(x_i) - y_i], \tag{6}$$

where $\alpha(x_i) = 1 + [x_i]^+$ and $\beta(x_i) = [x_i]^+(1 + [x_i]^+)$. Thus the slow conductance $y_i$ is gated by a voltage-dependent rate term $\alpha(x_i)$ and approaches a voltage-dependent asymptote $\beta(x_i)$, both of which increase with voltage $x_i$.

The notation in (5) and (6) is consistent with the following biophysical interpretations of equations (1) and (2). Variable $x_i$ computes the activity, or potential, of an excitatory neuron, or neuron population, and $y_i$ is the activity, or potential, of an inhibitory interneuron, or interneuron population. Equations (1) and (2) may also be given an intracellular interpretation wherein $y_i$ controls a slow inhibitory intracellular conductance, rather than a separate inhibitory interneuron. As noted above, the excitatory and inhibitory activities obey a membrane or, shunting, equation (Grossberg, 1982; Hodgkin, 1964). The excitatory and inhibitory feedback signals $f(x_i)$ and $g(x_j)$, respectively, are rectified sigmoids, as in (4). Each $x_i$ excites only itself, whereas inhibition may occur via the lateral inhibitory coupling terms $D_{ij}g(y_j)$ in (1). The input terms $I_i$ represent volitional input signals. When only a scalar GO signal perturbs the network, all $I_i = I$.

Oscillations in such a network occur only when the inhibitory interneuronal rate $E$ in (2) is sufficiently small. Indeed, when $E$ is sufficiently large, $y_i$ tracks $x_i$ in (2). Then $y_i$

may be replaced by $[x_i]^+(1+[x_i]^+)$ in (1), and the network (1) approaches an equilibrium point under very general conditions on $f$ and $g$ if the coefficients $D_{ij}$ are symmetric (Cohen and Grossberg, 1983; Hirsch, 1989). Addition of the shunting term $-y_i[x_i]^+$ in (2), that makes $\alpha(x_i)$ voltage-dependent in (6), is needed to generate some gait transitions, such as the transition from the walk to the run in bipeds that is simulated in Pribe, Grossberg, and Cohen (1996).

## 4. Simulations of Bidirectional Phase Reversals as the GO Signal Increases

As noted in Section 1, coordinated finger movements can switch from anti-phase to in-phase oscillations as oscillation frequency increases. It is known, more generally, that interlimb oscillations can bifurcate between anti-phase and in-phase oscillations in either direction. As in the case of finger movements, Grillner and Zangger (1979) have shown that, in the deafferented spinal cat, hind limbs transfer from anti-phase to in-phase movement as a function of increasing level of stimulation. However, the phase relationship of the transverse limbs of a free roving quadruped can switch from in-phase movement to anti-phase movement with increasing speed, as when a switch from a trot to a pace occurs; see Pribe, Grossberg, and Cohen (1996). How can a *single* CPG generate transitions both from in-phase to anti-phase movements and from anti-phase to in-phase movements as the oscillation frequency increases with increases in volitional signals, particularly a single GO signal?

For this to occur in a quadruped, control of four limbs or movement channels is required. Herein, we first show how it can happen in a simpler two-channel CPG, as in Figure 4, where $I_1 = I_2 = I =$ the GO signal. Such a two-channel CPG network can exhibit both in-phase and anti-phase oscillations such that anti-phase oscillations precede in-phase, or vice versa, in different parameter ranges (Figure 5) as the oscillation frequency increases. As illustrated in the computer simulation of Figure 6, for fixed inhibitory cross-coupling strengths $D_{ij}$, $i \neq j$, an increase in the self-inhibitory coupling strength $D_{ii}$ tends to move the system from in-phase→anti-phase transitions to anti-phase→in-phase transitions as the GO signal $I$ is parametrically increased. In addition, there is a tendency in some parameter ranges for anti-phase oscillations to occur at extreme values of $I$ which bracket the intermediate $I$ values at which in-phase oscillations occur; see Figure 5.

Figure 5

Figures 7 and 8 illustrate the temporal response of the oscillator to different levels of arousal $I$. The same values of $I$ are used in both Figures. Each figure illustrates the effect of the inhibitory coefficients, chosen as in Figures 6A and 6B, respectively, as $I$ is increased. In Figure 7, in-phase oscillations (Figures 7A–C) precede anti-phase oscillations (Figures 7D–E) as oscillation frequency increases. In Figure 8, anti-phase oscillations (Figures 8A–B) precede in-phase oscillations (Figures 8C–E). Note the sharp peaks in the anti-phase waveform in Figure 8A and 8B and compare these with the broad plateau waveforms of the anti-phase waveform of Figure 7D and 7E. In our simulations, anti-phase oscillations which precede in-phase oscillations consistently tend to have sharp peaks and those which occur after in-phase oscillations tend to be plateau-like. This property illustrates that, in addition to phase and frequency, waveform shape could be used to differentiate and control transitions between different gaits which have the same relative phase, but different qualitative behavior. This property is used in Pribe, Grossberg, and Cohen (1996) to simulate differences between a human walk and run, and an elephant amble and walk. This analysis suggests that anti-phase

waveform shape may be a useful observable index for where the system lies in parameter space.

Figure 6

## 5. Oscillations of a Two-Channel CPG with Asymmetric Parameters

The two-channel CPG model in Figure 4 is defined by the equations:

$$\frac{d}{dt}x_1 = -Ax_1 + (B - x_1)[f(x_1) + I_1] - (C + x_1)[D_{11}g(y_1) + D_{12}g(y_2)], \tag{7}$$

$$\frac{d}{dt}y_1 = E[(1 - y_1)[x_1]^+ - y_1], \tag{8}$$

$$\frac{d}{dt}x_2 = -Ax_2 + (B - x_2)[f(x_2) + I_2] - (C + x_2)[D_{21}g(y_1) + D_{22}g(y_2)], \tag{9}$$

and

$$\frac{d}{dt}y_2 = E[(1 - y_2)[x_2]^+ - y_2]. \tag{10}$$

In such a network, each channel excites itself via terms $f(x_i)$ and inhibits the other channel, via terms $D_{ij}g(y_j)$, as well as itself via term $D_{ii}g(y_i)$. A casual inspection of such an opponent organization between channels might have lead to the erroneous conclusion that it can, at best, generate anti-phase oscillations. As noted in Figures 6–8, such a $G^3$ model can produce both in-phase and anti-phase oscillations as the GO signal $I = I_1 = I_2$ is increased, and can do so in either order.

Figure 7

Our analysis of how this can happen was based on the mathematical results of Ellias and Grossberg (1975), who studied a similar system with symmetric inhibitory coupling ($D_{11} = D_{22}$ and $D_{12} = D_{21}$), uniform initial data ($x_i(0) = x > 0$ and $y_i(0) = y > 0$), and uniform inputs ($I_i = I$). By symmetry, $x_1 \equiv x_2 \equiv x$ and $y_1 \equiv y_2 \equiv y$ for all time, so the system behaves like the one-channel network shown in Figure 9. Ellias and Grossberg (1975) used the Hopf bifurcation theorem to prove the existence of an oscillatory regime at intermediate values of $I$ for the one-channel network, and thus the existence of in-phase oscillations in the two-channel symmetric network. The one-channel network and two-channel symmetric networks approach equilibrium at smaller and larger $I$ values.

Figure 8

To design a CPG with both in-phase and anti-phase oscillations, one can use a one-channel oscillator as a building block for constructing a two-channel network that reduces to the one-channel oscillator when all initial data and parameters are symmetric. To accomplish this, choose the inhibitory weights $D_{ij}$ in (7) and (9) so that $\sum_j D_{ij} = D$, where $D$ equals the inhibitory coefficient of the one-channel network

$$\frac{d}{dt}x = -Ax + (B - x)[f(x) + I] - (C + x)Dg(y) \tag{11}$$

and

$$\frac{d}{dt}y = E[(1 - y)[x]^+ - y]. \tag{12}$$

Let $I$ in (11) be increased from the values at which there are one-channel in-phase oscillations to values at which equilibrium is re-established. In the symmetric two-channel version of this network, the variables oscillate in-phase (viz, $x = x_1 = x_2$ and $y = y_1 = y_2$) until an $I$ is reached where they converge to a stable equilibrium point. One way to generate a system with both in-phase and anti-phase oscillations is to break the system's symmetry so that it can generate anti-phase oscillations when $x_1 \neq x_2$ and $y_1 \neq y_2$ (viz., "off the diagonal") at $I$ values that are either too small or too large to generate symmetric in-phase oscillations.

Figure 9

Several neurophysiologically plausible operations can be used to break symmetry. The first operation makes a slightly asymmetric choice of inhibitory coefficients $D_{ij}$, as occurs in the bilaterally asymmetric organization of many neural systems (Bradshaw, 1989). Such asymmetric coefficients can bias the system towards generating specific asymmetric gaits. The second operation uses the GO signal, $I$, to break symmetry. This can be done in two ways: (1) Choose one GO input stronger than the other; that is, let $I_1 = I$ in (7) and $I_2 = I + \delta$ in (9). (2) Choose inputs with equal amplitudes but slightly asynchronous onset times; that is, let $I_1(t) = I$ and $I_2(t) = I(t-\delta)$. Mechanism (1) produces a spatial asymmetry in the oscillator, mechanism (2) a temporal asymmetry. Both asymmetries are small enough to be caused by random variations in network parameters during morphogenesis, if not more pervasive asymmetries in neural organization. The temporal asymmetry automatically scales with the GO amplitude $I$. Such a temporal asymmetry can, for example, be robustly designed into the network using an extra interneuron to the cells with delayed signals. We used a temporal asymmetry in the simulations of the two-channel oscillator shown in Figures 6, 7, and 8 where the lag $\delta = 0.001$. As shown in Figure 5, this small asynchrony in the GO arrival time produces anti-phase oscillations for many values of the parameters. The only parameters that were varied in these simulations were the inhibitory coefficients ($D_{ii}$ and $D_{ij}$) and the arousal level $I$. It is shown in Pribe, Grossberg, and Cohen (1996) that temporal, but not spatial, asymmetry is capable of controlling rapid gait transitions in some regimes. Our results thus suggest that measurements which test for the bilateral asymmetry of GO onset times be undertaken in the CPGs that control oscillatory movements.

## 6. Bimanual Coordination at Variable Frequencies

Using these results as a foundation, we simulated a large body of behavioral data as emergent properties of the CPG, notably the four properties summarized in Section 1. The CPG reliably reproduces all four effects in our simulations. In order to simulate these four properties, the model was presented with a pulsed wave anti-phase oscillatory input to each channel in place of a single arousal or GO signal, as shown in Figure 2A. These pulsed inputs represent the descending volitional commands to move the fingers as required. The square waves were either equal to a constant input level when on, or set to zero when off. The input level and the duration of the "on" portion of the signal were held constant for each of the simulations. For each simulation, only the frequency of these pulses was varied. The duration of the "on" portion of the signals was 2.0 in all simulations. Shorter duration signals did not reliably produce oscillations in both channels. In order to generate Figure 1B, we computed, for 145 points, the relative phases of the output signals using the times at which they exceeded a threshold. As the frequency was varied, the model showed a switch from anti-phase (Figure 2B) to in-phase (Figure 2D) oscillations. As in the data, it did not show the reverse transition in response to in-phase inputs (Figure 3). The system also

exhibited fluctuations between the anti-phase and in-phase regimes (Figure 2C). It should also be noted that parameters can be chosen so that the system locks into the anti-phase pattern independent of the phase of the pulsed input pattern.

## 7. Discussion

The opponent CPG model shows how a ubiquitously occurring neural design—a recurrent on-center off-surround network whose cells obey membrane equations—can give rise to activation patterns characteristic of coordinated rhythmic movements. The patterning of inputs organizes the network to behave as if it possesses special linkages between particular joints, whereas in reality, the inhibitory connections can be widespread and nonspecific. The model hereby illustrates how neural interactions can coordinate novel movement combinations that are not specified in the wiring diagram of the brain.

The anatomical location of the network that is rate-limiting in transforming the volitional input pulses into oscillations which exhibit the four properties summarized in Section 1 is not yet established. It could, in principle, be located anywhere on the pathway from the motor cortex to the spinal cord. In this regard, Jacobs and Donoghue (1991) have reported widespread inhibitory interactions among somatotopic representations in motor cortex that are consistent with model properties. If these representations are the generators of the observed pattern, then they would provide an example of a cortical representation that may be transformed into a CPG by the patterning of its inputs.

## REFERENCES


Bradshaw, J.L. (1989). **Hemispheric specialization and psychological function**. New York: John Wiley and Sons.

Bullock, D. and Grossberg, S. (1988). Neural dynamics of planned arm movements: Emergent invariants and speed-accuracy properties during trajectory formation. *Psychological Review*, **95**, 49–90.

Bullock, D. and Grossberg, S. (1991). Adaptive neural networks for control of movement trajectories invariant under speed and force rescaling. *Human Movement Science*. **10**, 3–53.

Cohen, M.A. and Grossberg, S. (1983). Absolute stability of global pattern formation and parallel memory storage by competitive neural networks. *IEEE-SMC*, **13**, 815–826.

Dudel, J. and Kuffler, S.W. (1961). Presynaptic inhibition at the crayfish neuromuscular junction. *Journal of Physiology*, **155**.

Ellias, S. and Grossberg, S. (1975). Pattern formation, contrast control, and oscillations in the short term memory of shunting on-center off-surround networks. *Biological Cybernetics*, **20**, 69–98.

Grillner, S. and Zangger, P. (1979). On the central pattern generation of locomotion in the low spinal cat. *Experimental Brain Research*, **34**, 241–261.

Grossberg, S. (1982). **Studies of mind and brain**. Boston, MA: Reidel Press.

Hirsch, M.W. (1989). Convergent activation dynamics in continuous time networks. *Neural Networks*, **2**, 331–349.

Hodgkin, A.L. (1964). **The conduction of the nervous impulse**. Liverpool, England: Liverpool University Press.

Jacobs, K.M. and Donoghue, J.P. (1991). Reshaping the cortical motor map by unmasking latent intracortical connections. *Science*, **251**, 944–947.

Kaczmarek, L. and Levitan, I.B. (1987). **Neuromodulation**. London, England: Oxford University Press.

Kandel, E.R., Schwartz, J.H., and Jessell, T.M. (1991). **Principles of neural science, 3rd edition**. New York: Elsevier Science Publishing.

Kelso, J.A.S. (1981). On the oscillatory basis of movement. *Bulletin of the Psychonomic Society*, **18**, 63.

Kelso, J.A.S. (1984). Phase transitions and critical behavior in human bimanual coordination. *Am. J. Physiol., Reg. Integ. Com.*, **15**, R1000-R1004.

Kelso, J.A.S. and Scholz, J.P. (1985). Cooperative phenomena in biological motion. In H. Haken (Ed.) **Complex systems: Operational approaches in neurobiology, physical systems, and computers**. Berlin: Springer, 124–149.

Kelso, J.A.S., Scholz, J.P., and Schöner, G. (1988). Dynamics governs switching among patterns of coordination in biological movement. *Physics Letters A.*, **134**, 8–12.

Kuffler, S. (1953). Discharge patterns and functional organization of mammalian retina. *Journal of Neurophysiology*, **16**, 37–68.

Pearson, K.G. (1993). Common principles of motor control in vertebrates and invertebrates. *Annual Review of Neuroscience*, **16**, 256–297.

Petzold, L.R. and Hindmarsh, H. (1987). LSODA Numerical Integration Package. *Technical Report*, Lawrence Livermore National Laboratory, Livermore, California.

Pribe, C., Grossberg, S., and Cohen, M. (1996). Neural control of interlimb oscillations, II: Biped and quadruped gaits and bifurcations. Technical Report CAS/CNS-TR-94-022, Boston, MA: Boston University. Submitted for publication.

Ratliff, F. (1965). **Mach bands: Quantitative studies on neural networks in the retina.** New York: Holden-Day.

Schöner, G., Jiang, W.Y., and Kelso, J.A.S. (1990). A synergetic theory of quadrupedal gaits and gait transitions. *Journal of Theoretical Biology*, **142**, 359–391.

Schöner, G. and Kelso, J.A.S. (1988). Dynamic pattern generation in behavioral and neural systems, *Science*, **239**, 1513–1520.

Tuller, B. and Kelso, J.A.S. (1989). Environmentally-specified patterns of movement coordination in normal and split-brain subject. *Experimental Brain Research*, **75**, 306–316.

Von Békésy, G. (1968). Mach- and Hering-type lateral inhibition in vision. *Vision Research*, **8**, 1483–1499.

Yamanishi, J., Kawato, M., and Suzuki, R. (1980). Two coupled oscillators as a model for the coordinated finger tapping by both hands. *Biological Cybernetics*, **37**, 219–225.

Yuasa, H. and Ito, M. (1990). Coordination of many oscillators and generation of locomotory patterns. *Biological Cybernetics*, **63**, 177–184.

## FIGURE CAPTIONS

**Figure 1:** (A) An example illustrating both the "seagull" effect and the tendency to slip from intermediate phase relationships toward purely in-phase and anti-phase relationships. [Reprinted with permission from Yamanishi, Kawato, and Suzuki (1980).] (B) The model exhibits the "seagull" effect: Intermediate phase relationships are more variable than purely in-phase or purely anti-phase relationships. The standard deviation of the observed relative phases is plotted against the required relative phase. The model exhibits the tendency to slip from intermediate phase relationships toward purely in-phase and anti-phase relationships. This plot shows the mean of the (observed–required) phase. There are 145 points per mean.

**Figure 2:** Bifurcation from anti-phase to in-phase oscillation in response to anti-phase inputs of increasing frequency. The anti-phase inputs $I_i$ in (A) give rise to the anti-phase oscillation in (B). The input frequency in (A) is low, .1 pulses per unit time (a pulse turns on every 10 time units); (C) at intermediate input frequencies (0.65), fluctuations occur; (D) at high input frequencies (0.85), in-phase oscillations obtain. $A = 1.0$, $B = 1.1$, $C = 2.5$, $D_{ii} = 0.8$, $D_{ij} = 0.45$, $i \neq j$, $E = 1.0$, $F_1 = 9.0$, $G_1 = 3.9$, $F_2 = 0.5$, $G_2 = 0.5$. The duration of each pulse was 0.75. The integration step size was 0.001. The initial conditions were reset to zero before each run. The LSODA numerical integration package (Petzold and Hindmarsh, 1987) provided accurate numerical integration throughout. LSODA "solves systems $\frac{dy}{dt} = f$ with full or bounded Jacobian when the problem is stiff, but it automatically selects between non-stiff (Adams) and stiff (BDF) methods. It uses the non-stiff method initially, and dynamically monitors data in order to decide which method to use." (lsoda. netlib documentation.).

**Figure 3:** As the frequency of the in-phase inputs is parametrically increased, the oscillator output also stays in-phase: No bifurcations occur. The in-phase input shown in $(A)$ produces the output shown in $(B)$. The in-phase output for inputs with higher frequency in-phase oscillations are shown in $(C)$ and $(D)$. The parameters and input frequencies are as in Figure 2, except the input is always in-phase.

**Figure 4:** The CPG is defined by a recurrent on-center off-surround network whose cells obey membrane, or shunting, equations. See text for details.

**Figure 5:** A plot of the oscillatory regions at different arousal levels for various choices of inhibitory coefficients. The relative phases were determined automatically by an algorithm which compared the relative times when the channels exceeded an output threshold, set here to 0.35. The initial conditions were not reset to 0 as $I$ increased, but only at the beginning of each run, when the inhibitory coefficients were changed. The other parameters ($A = 1.0$, $B = 1.1$, $C = 2.5$, $E = 1.0$, $F_1 = 9.0$, $G_1 = 3.9$, $F_2 = 0.5$, $G_2 = 0.5$) were chosen as in Figure 2.

**Figure 6:** Frequency plots for: (A) in-phase to anti-phase oscillations ($D_{ii} = 0.8$, $D_{ij} = 0.45$) and (B) anti-phase to in-phase oscillations ($D_{ii} = 1.3$, $D_{ij} = 0.55$) as $I$ increases. The initial conditions were reset at each $I$ increment and other parameters are as in Figure 4. The system approaches an equilibrium point between its in-phase and anti-phase regimes in (A).

**Figure 7:** In-phase and anti-phase oscillations at different arousal levels with inhibitory coefficients fixed at $D_{ii} = 0.8$, $D_{ij} = 0.45$, as in Figure 6A. The in-phase oscillations occur

for lower values of $I$ than do the anti-phase oscillations. $I = .1, .25, .5, .95$, and 1.15 in (A)–(E), respectively. Other parameters are as in Figure 5. Because LSODA provides variable step size integration, any jagged appearance in the figures is an artifact of the output times chosen and not of the time steps used in the integration.

**Figure 8:** In-phase and anti-phase oscillations at different arousal levels with inhibitory coefficients fixed at $D_{ii} = 1.3$, $D_{ij} = 0.55$, as in Figure 6B. The anti-phase oscillations occur for lower values of $I$ than do the in-phase oscillations. Note the bimodal anti-phase waveforms in (A) and (B). $I = .1, .25, .5, .95$, and 1.15 in (A)–(E), respectively, as in Figure 6. Other parameters are as in Figure 5.

**Figure 9:** The one-channel Ellias-Grossberg model undergoes Hopf bifurcations when the arousal level, or GO signal, is varied. A global equilibrium is approached at both low and high arousal levels. Oscillations occur at intermediate arousal levels. See Ellias and Grossberg (1975) for details.

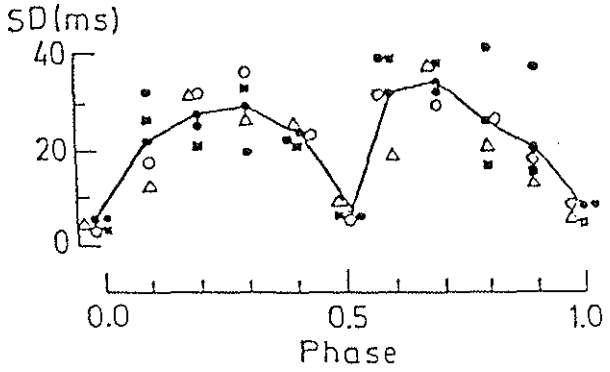
SD(ms)
40
20
0
0.0
0.5
1.0
Phase

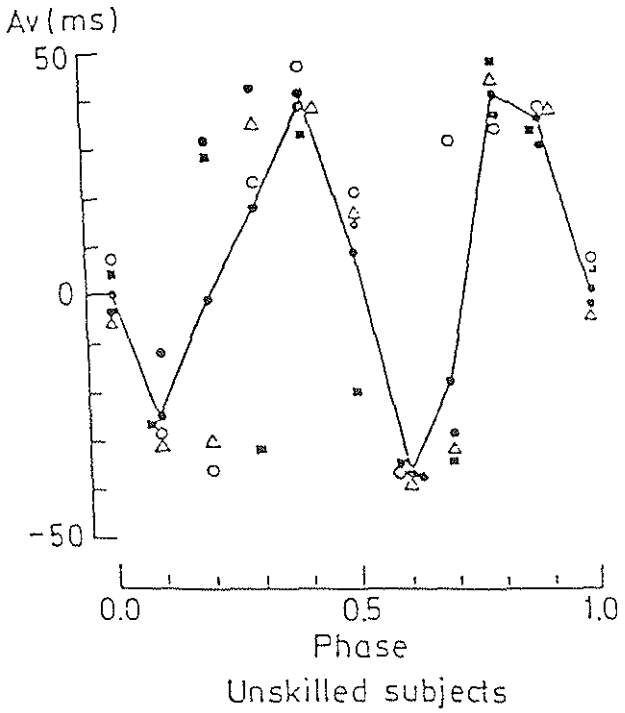
Av(ms)
50
0
-50
0.0
0.5
1.0
Phase
Unskilled subjects

(A)

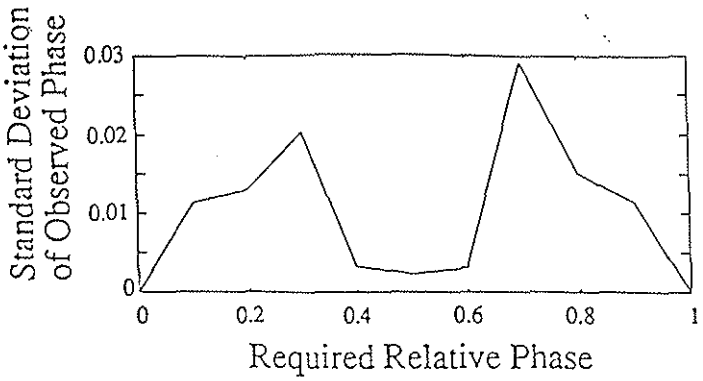
Standard Deviation of Observed Phase
0.03
0.02
0.01
0
0
0.2
0.4
0.6
0.8
1
Required Relative Phase

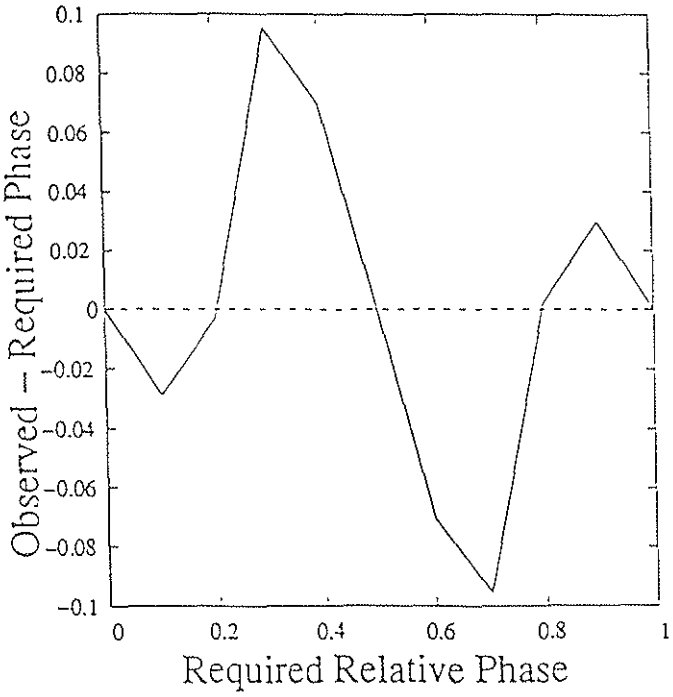
Observed – Required Phase
0.1
0.08
0.06
0.04
0.02
0
-0.02
-0.04
-0.06
-0.08
-0.1
0
0.2
0.4
0.6
0.8
1
Required Relative Phase

(B)

Figure 1

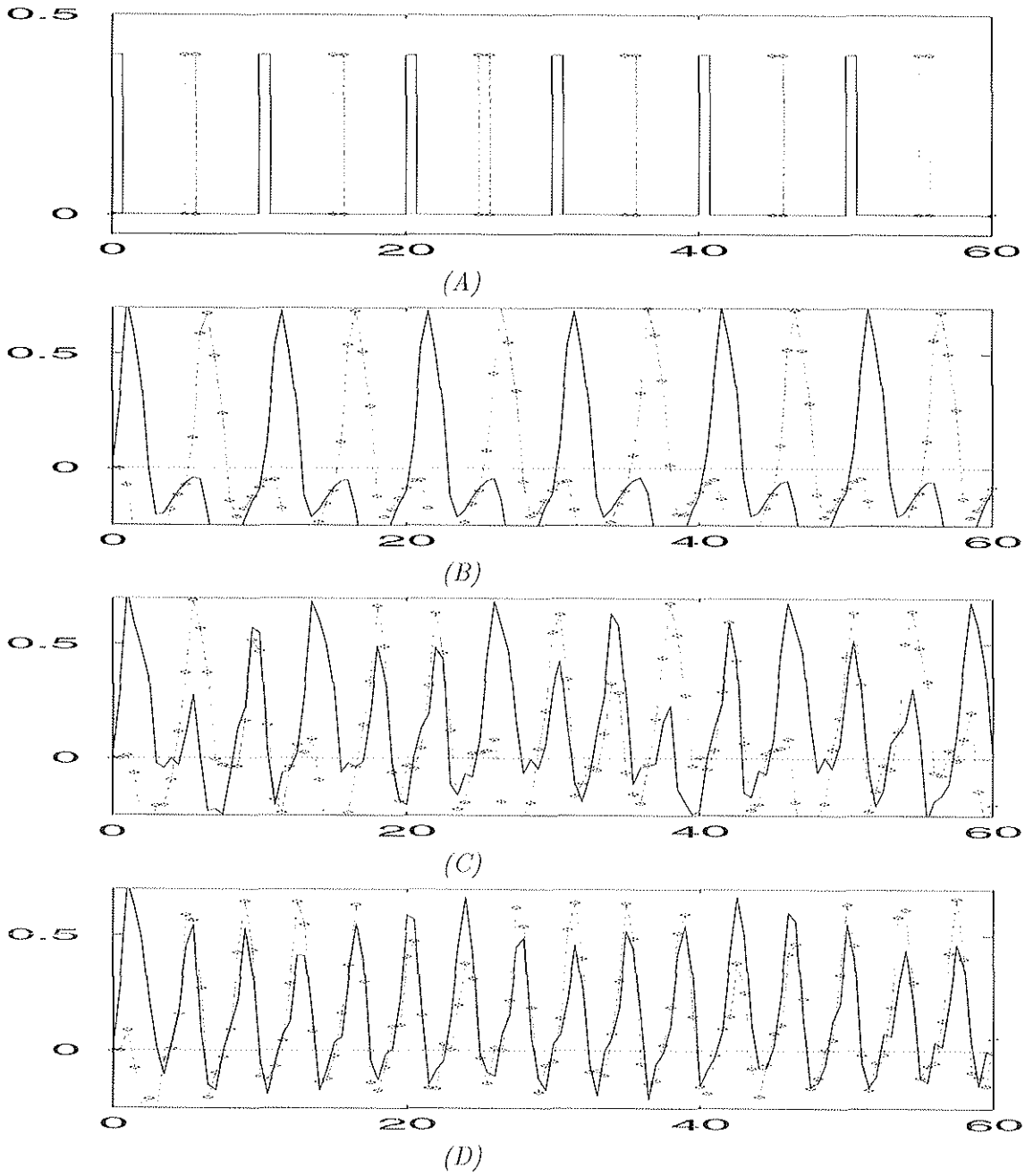


Figure 2

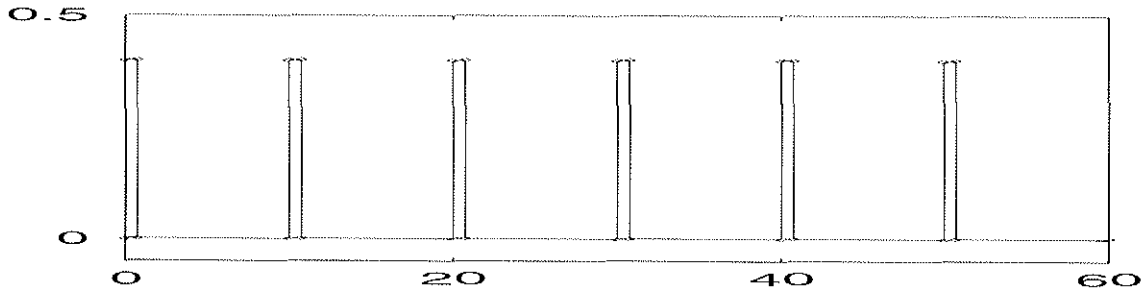


(A)

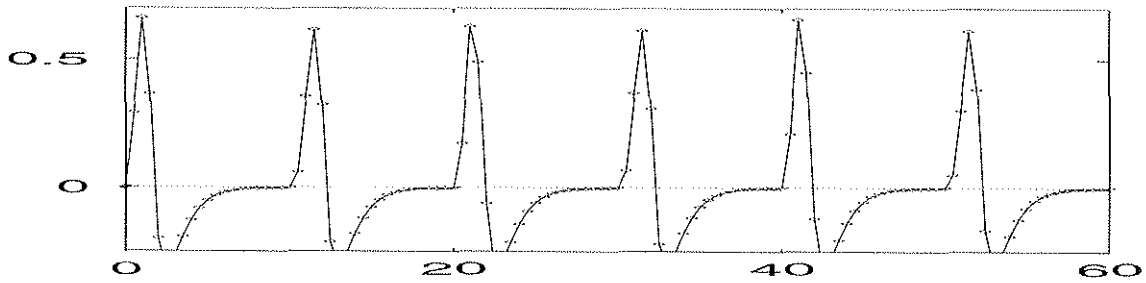


(B)

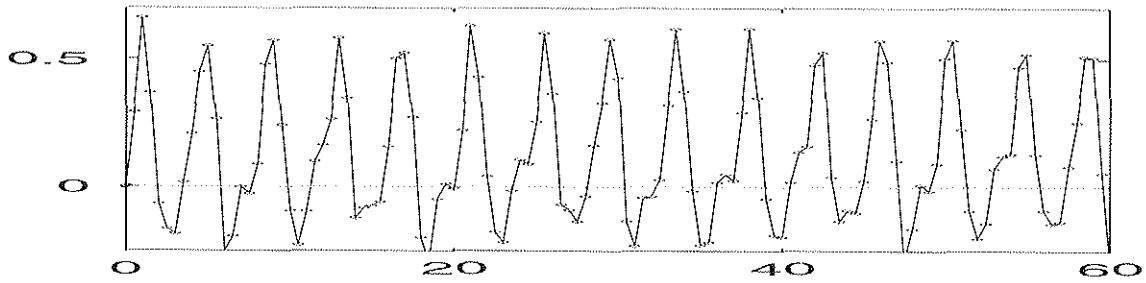


(C)

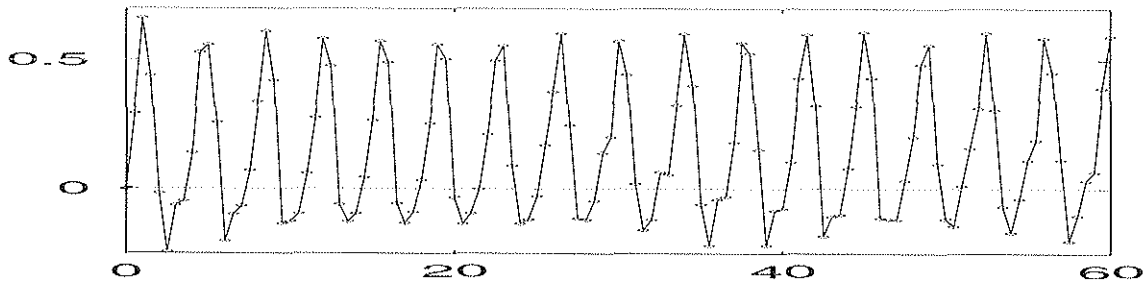


(D)

Figure 3

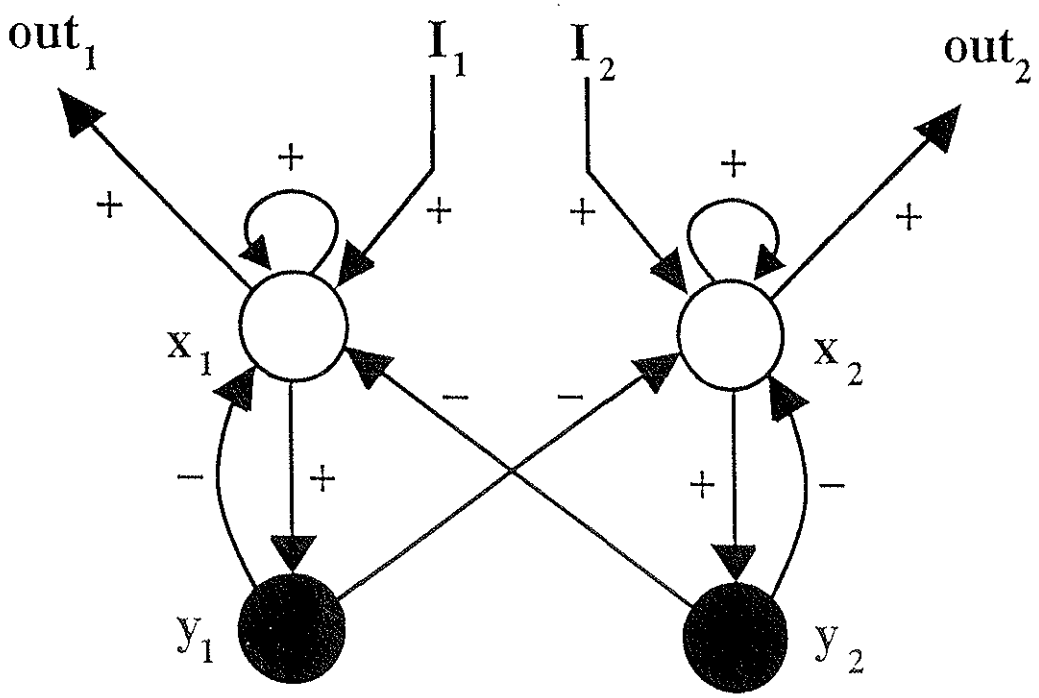


Figure 4

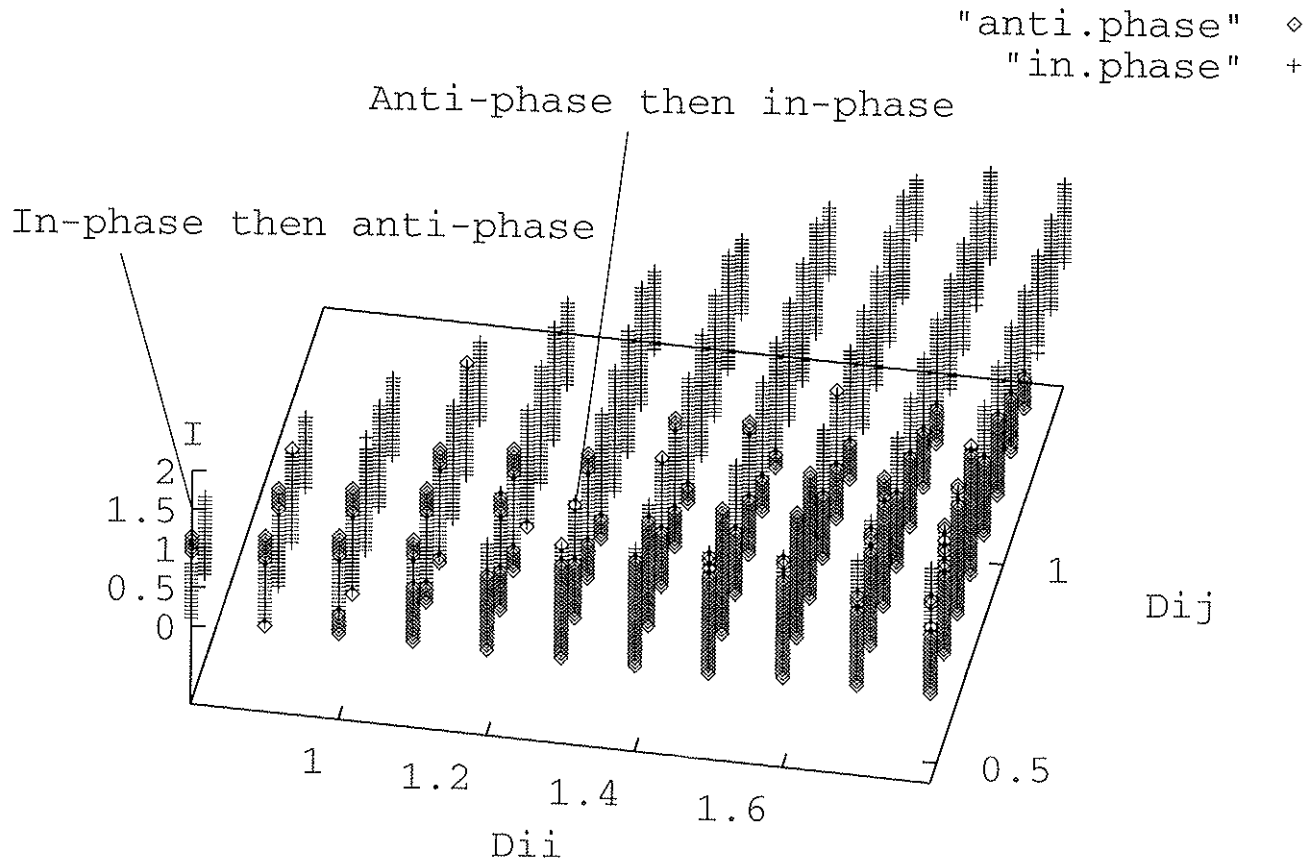
"anti.phase" ◇
"in.phase" +
Anti-phase then in-phase
In-phase then anti-phase
I
2
1.5
1
0.5
0
1
1.2
1.4
1.6
Dii
1
0.5
Dij

Figure 5

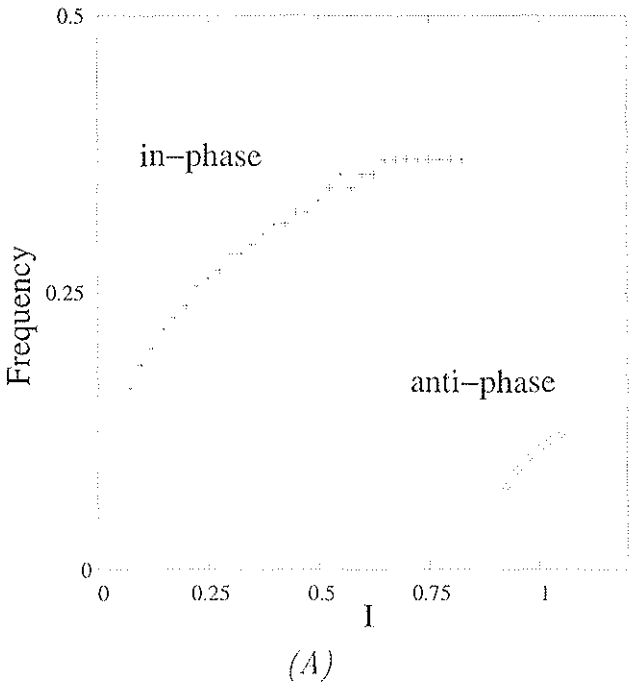
0.5
0.25
0
Frequency
in–phase
anti–phase
0
0.25
0.5
0.75
1
I

*(A)*

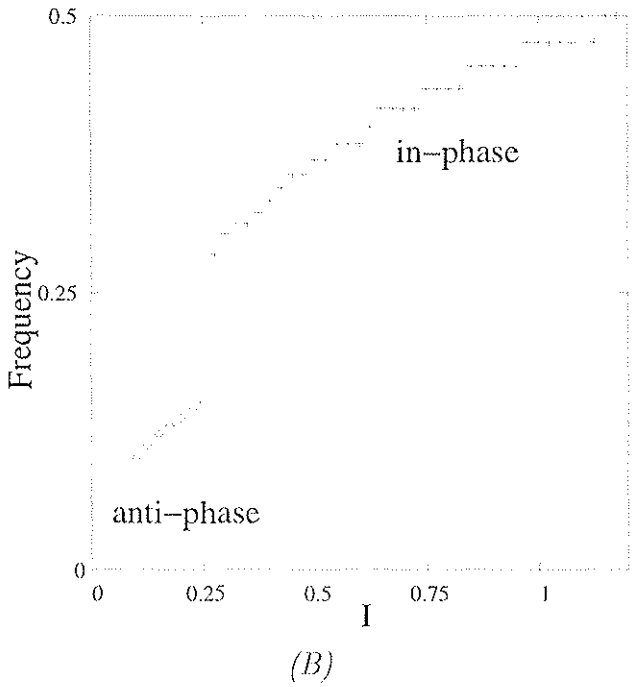
0.5
0.25
0
Frequency
in–phase
anti–phase
0
0.25
0.5
0.75
1
I

*(B)*

Figure 6

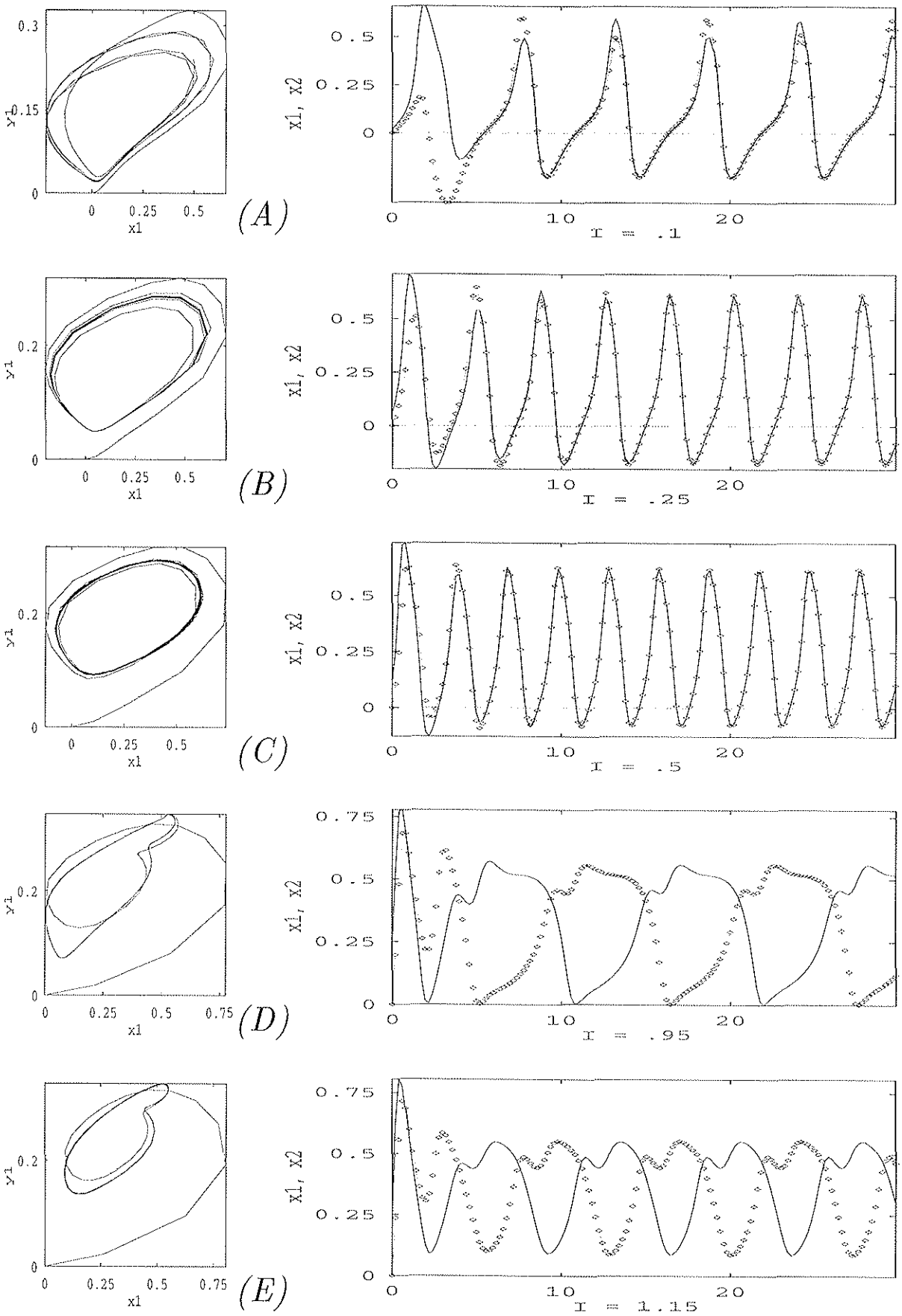


Figure 7

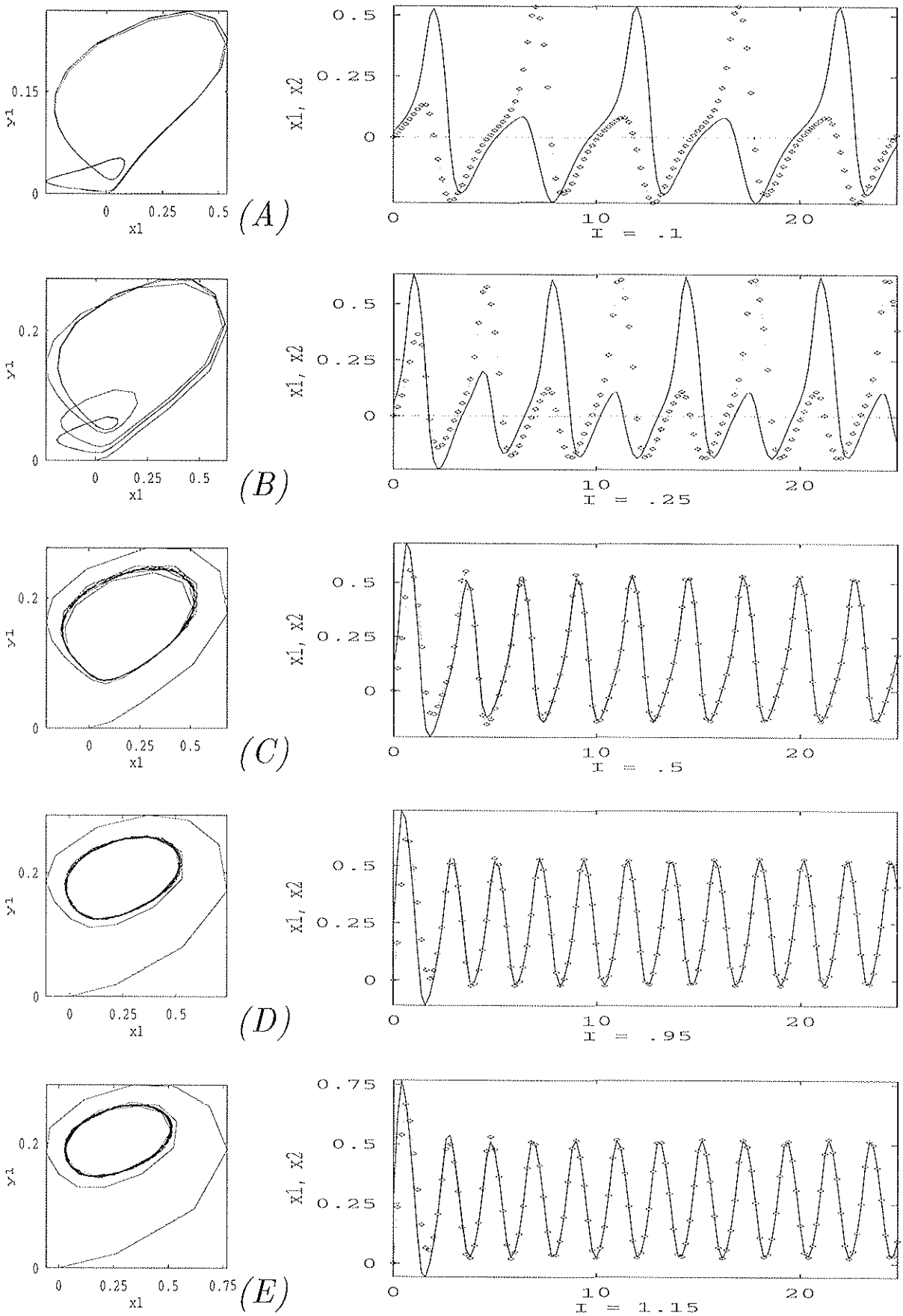
y1
x1
0.15
0
0.25
0.5
(A)
x1, x2
0.5
0.25
10
20
I = .1
0.2
(B)
I = .25
(C)
I = .5
(D)
I = .95
0.75
(E)
I = 1.15

Figure 8

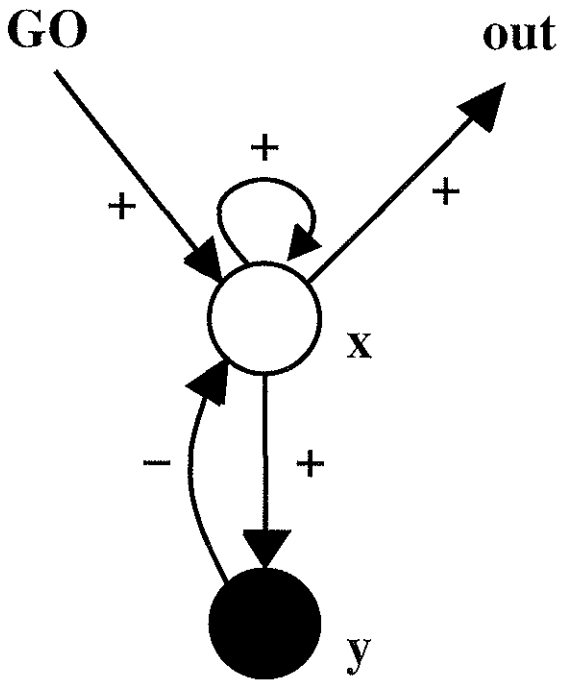


Figure 9